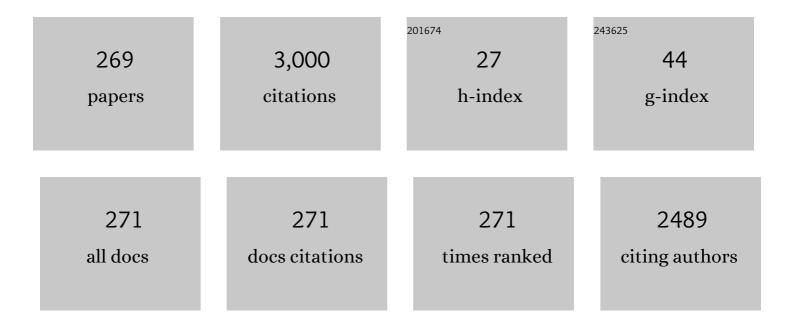
List of Publications by Year in descending order

Source: https://exaly.com/author-pdf/8522405/publications.pdf Version: 2024-02-01



#	Article	IF	CITATIONS
1	Engineering 1/f noise in porous silicon thin films for thermal sensing applications. Microporous and Mesoporous Materials, 2021, 324, 111302.	4.4	11
2	Photostriction actuation of silicon-germanium bilayer cantilevers. Journal of Applied Physics, 2019, 125, .	2.5	5
3	Abnormal auditory mismatch fields in adults with autism spectrum disorder. Neuroscience Letters, 2019, 698, 140-145.	2.1	22
4	Delayed Auditory Evoked Responses in Autism Spectrum Disorder across the Life Span. Developmental Neuroscience, 2019, 41, 223-233.	2.0	19
5	Quantifying the Effects of 16p11.2 Copy Number Variants on Brain Structure: A Multisite Genetic-First Study. Biological Psychiatry, 2018, 84, 253-264.	1.3	56
6	Large-Area MEMS Tunable Fabry–Perot Filters for Multi/Hyperspectral Infrared Imaging. IEEE Journal of Selected Topics in Quantum Electronics, 2017, 23, 45-52.	2.9	27
7	An optical MEMS cross-bar switch. , 2016, , .		0
8	MEMS-Based Tunable Fabry–Perot Filters for Adaptive Multispectral Thermal Imaging. Journal of Microelectromechanical Systems, 2016, 25, 227-235.	2.5	17
9	Preparation and Characterization of Cerium Substituted Bismuth Dysprosium Iron Garnets for Magneto-Optic Applications. IEEE Transactions on Magnetics, 2016, 52, 1-4.	2.1	4
10	Effect of CdS Processing Conditions on the Properties of CdS/Si Diodes and CdS/CdTe Thin-Film Solar Cells. IEEE Journal of Photovoltaics, 2015, 5, 1783-1790.	2.5	6
11	Substrate heating effects on properties of CdS thin films prepared by thermal evaporation for photovoltaic applications. , 2015, , .		1
12	Silicon-Air-Silicon Distributed Bragg Reflectors for Visible and Near Infrared Optical MEMS. Journal of Microelectromechanical Systems, 2015, 24, 1245-1247.	2.5	5
13	Ge/ZnS-Based Micromachined Fabry–Perot Filters for Optical MEMS in the Longwave Infrared. Journal of Microelectromechanical Systems, 2015, 24, 2109-2116.	2.5	13
14	Large-Area MEMS-Based Distributed Bragg Reflectors for Short-Wave and Mid-Wave Infrared Hyperspectral Imaging Applications. Journal of Microelectromechanical Systems, 2015, 24, 2136-2144.	2.5	11
15	Characterization and Modeling of Photostriction in Silicon Cantilevers Fabricated on Silicon-on-Insulator Substrates. Journal of Microelectromechanical Systems, 2015, 24, 182-191.	2.5	2
16	MBE Growth of Mid-wave Infrared HgCdTe Layers on GaSb Alternative Substrates. Journal of Electronic Materials, 2015, 44, 3180-3187.	2.2	37
17	Investigation of ICPECVD Silicon Nitride Films for HgCdTe Surface Passivation. Journal of Electronic Materials, 2015, 44, 2990-3001.	2.2	13
18	Suspended Large-Area MEMS-Based Optical Filters for Multispectral Shortwave Infrared Imaging Applications. Journal of Microelectromechanical Systems, 2015, 24, 1102-1110.	2.5	4

#	Article	IF	CITATIONS
19	Optimization of ICPCVD Amorphous Silicon for Optical MEMS Applications. Journal of Microelectromechanical Systems, 2015, 24, 1998-2007.	2.5	6
20	On-chip read-out of picomechanical motion under ambient conditions. Nanoscale, 2015, 7, 1927-1933.	5.6	14
21	Investigation of crystallized germanium thin films and germanium/silicon heterojunction devices for optoelectronic applications. Materials Science in Semiconductor Processing, 2015, 30, 413-419.	4.0	9
22	Microcantilevers as a platform for the detection of hydrogen. , 2014, , .		0
23	Strain simulation and MBE growth of CdTe on GaSb substrates. , 2014, , .		0
24	Deposition heating effect on CdS thin films prepared by thermal evaporation for CdTe solar cells. , 2014, , .		4
25	Targeted machining during MEMS device fabrication using PDMS microfluidic cassettes. , 2014, , .		0
26	Characterisation of SiN <inf>x</inf> -HgCdTe interface in metal-insulator-semiconductor structure. , 2014, , .		0
27	High Resolution Position Monitoring of Suspended MEMS towards Biological and Chemical Sensors. Materials Research Society Symposia Proceedings, 2014, 1659, 9-14.	0.1	0
28	An optically resonant position read-out system for MEMS gas sensors. , 2014, , .		0
29	Characterization of mechanical, optical and structural properties of bismuth oxide thin films as a write-once medium for blue laser recording. Materials Research Society Symposia Proceedings, 2014, 1633, 87-92.	0.1	1
30	Recent developments towards low-cost MEMS spectrometers. , 2014, , .		2
31	Tailoring Anchor Etching Profiles During MEMS Release Using Microfluidic Sheathed Flow. Journal of Microelectromechanical Systems, 2014, 23, 918-926.	2.5	1
32	Investigation of Cerium-Substituted Europium Iron Garnets Deposited by Biased Target Ion Beam Deposition. IEEE Transactions on Magnetics, 2014, 50, 1-7.	2.1	13
33	GaSb: A New Alternative Substrate for Epitaxial Growth of HgCdTe. Journal of Electronic Materials, 2014, 43, 2788-2794.	2.2	43
34	Process Control of Cantilever Deflection for Sensor Application Based on Optical Waveguides. Journal of Microelectromechanical Systems, 2013, 22, 569-579.	2.5	13
35	Depth Profiling of Electronic Transport Parameters in n-on-p Boron-Ion-Implanted Vacancy-Doped HgCdTe. Journal of Electronic Materials, 2013, 42, 3108-3113.	2.2	25
36	A novel technique for degenerate p-type doping of germanium. Solid-State Electronics, 2013, 89, 146-152.	1.4	9

#	Article	IF	CITATIONS
37	Macromodel for the transient simulation of electrostatically actuated fixed-fixed beams. , 2013, , .		0
38	Optical actuation of silicon cantilevers: modelling and experimental investigation. , 2013, , .		0
39	Targeted sacrificial layer etching for MEMS release using microfluidic channels. , 2013, , .		0
40	Long-wavelength infrared Fabry-Perot etalon for multi-spectral thermal imaging. , 2013, , .		1
41	A versatile instrumentation system for MEMS-based device optical characterization. , 2013, , .		1
42	A silicon based surface micro-machined distributed Bragg reflector for MEMS spectroscopic applications. , 2013, , .		1
43	Optical read-out scheme based on grated waveguide cantilever cavity resonance for interrogation of cantilever sensor arrays. , 2012, , .		1
44	Demonstration of a method for detecting MEMS suspended beam height. , 2012, , .		0
45	A WDM Capable Integrated Optical Readout of a MEMS Sensor. Procedia Engineering, 2012, 47, 386-389.	1.2	Ο
46	Single crystal and amorphous Ge for use in stand-alone and thin film tandem solar cells. , 2012, , .		0
47	An optically resonant, grating-based technique for the sensitive detection of MEMS cantilever beam height. , 2012, , .		Ο
48	Integrated Resonant Optical Readout Applicable to Large Arrays of MEMS Beams. IEEE Photonics Technology Letters, 2012, 24, 2243-2246.	2.5	6
49	Mobility spectrum analysis of p-to-n type converted vacancy doped HgCdTe. , 2012, , .		Ο
50	Plasma annealing as an effective method for the crystallization of bismuth iron garnet films. , 2012, , .		0
51	Control of chemical composition of rare-earth substituted iron garnets using biased target deposition. , 2012, , .		1
52	Effect of FIB milling on MEMS SOI cantilevers. , 2012, , .		0
53	Tailoring anchor shape during release of MEMS microbeams using microfluidic flow. , 2012, , .		1
54	Characterization of low-temperature bulk micromachining of silicon using an SF ₆ /O ₂ inductively coupled plasma. Journal of Micromechanics and Microengineering, 2012, 22, 095005.	2.6	11

#	Article	IF	CITATIONS
55	Mechanisms of infrared photoluminescence in HgTe/HgCdTe superlattice. Journal of Applied Physics, 2012, 112, 063512.	2.5	37
56	Uniform Dispersion of Lanthanum Hexaboride Nanoparticles in a Silica Thin Film: Synthesis and Optical Properties. ACS Applied Materials & Interfaces, 2012, 4, 5833-5838.	8.0	27
57	Modeling and Design of a Thin-Film CdTe/Ge Tandem Solar Cell. Journal of Electronic Materials, 2012, 41, 2759-2765.	2.2	2
58	Model and Analysis of a High Sensitivity Resonant Optical Read-Out Approach Suitable for Cantilever Sensor Arrays. Journal of Lightwave Technology, 2012, 30, 1863-1868.	4.6	17
59	Recent developments towards low-cost miniaturized IR spectrometers for field applications. , 2012, , .		0
60	Development of an Alkaline-Compatible Porous-Silicon Photolithographic Process. Journal of Microelectromechanical Systems, 2011, 20, 418-423.	2.5	32
61	Vertical transport in InAs/GaSb type-II strained layer superlattices for infrared focal plane array applications. , 2011, , .		8
62	Recent advances in SWIR MEMS-based tunable Fabry-PÃ f Â $@$ rot microspectrometers. , 2011, , .		1
63	Photoresponse in photoconductor devices fabricated from HgTe-HgCdTe superlattices. Applied Physics Letters, 2011, 98, 043505.	3.3	2
64	Thermally induced damages of PECVD SiNx thin films. Journal of Materials Research, 2011, 26, 2552-2557.	2.6	3
65	On the accuracy of decay constant measurement by swept-cavity heterodyne cavity ringdown spectroscopy. Proceedings of SPIE, 2011, , .	0.8	0
66	Electrical type conversion of p-type HgCdTe induced by nanoimprinting. Journal of Applied Physics, 2011, 109, 096102.	2.5	2
67	Chemical resistance of porous silicon: photolithographic applications. Physica Status Solidi C: Current Topics in Solid State Physics, 2011, 8, 1847-1850.	0.8	12
68	A novel optical read-out technology for large arrays of micromachined cantilever sensors. , 2011, , .		0
69	Fabrication process for optically low loss Si cantilever waveguide. , 2011, , .		2
70	Performance predictions for monolithic thin-film CdTe/Ge tandem solar cells. , 2010, , .		0
71	A Study of Sidewall Effects in HgCdTe Photoconductors Passivated with MBE-Grown CdTe. Journal of Electronic Materials, 2010, 39, 1019-1022.	2.2	10
72	Nanoscratch-induced phase transformation of monocrystalline Si. Scripta Materialia, 2010, 63, 847-850.	5.2	86

#	Article	IF	CITATIONS
73	Electron magnetoresistance mobility in silicon-on-insulator layers using Kelvin's technique. Solid-State Electronics, 2010, 54, 1047-1050.	1.4	0
74	Capacitive sensing circuit for closed-loop control of wide tuning range microspectrometers. , 2010, , .		1
75	Dispersion of lanthanum hexaboride nanoparticles in water and in sol-gel silica arrays. , 2010, , .		0
76	Optical MEMS technologies for multi-spectral infrared sensors. , 2010, , .		0
77	Comparison of dynamic and static operation of a novel optical read-out technology for micromachined cantilever sensors. , 2010, , .		0
78	Nanoimprint induced electrical type conversion in HgCdTe. , 2010, , .		0
79	Elasto-plastic characterisation of low-temperature plasma-deposited silicon nitride thin films using nanoindentation. International Journal of Surface Science and Engineering, 2009, 3, 3.	0.4	6
80	MEMS-based Fabry-Perot microspectrometers for agriculture. Proceedings of SPIE, 2009, , .	0.8	5
81	Nanoscratch-induced deformation of single crystal silicon. Journal of Vacuum Science & Technology B, 2009, 27, 1374-1377.	1.3	48
82	Long-term environmental stability of residual stress of SiNx, SiOx, and Ge thin films prepared at low temperatures. Materials Science and Engineering B: Solid-State Materials for Advanced Technology, 2009, 163, 26-30.	3.5	11
83	Widely Tunable MEMS-Based Fabry–Perot Filter. Journal of Microelectromechanical Systems, 2009, 18, 905-913.	2.5	106
84	MEMS-based microspectrometer technologies for NIR and MIR wavelengths. Journal Physics D: Applied Physics, 2009, 42, 133001.	2.8	80
85	Electron magnetoresistance mobility in silicon on insulator layers using Kelvin's technique. , 2009, , .		0
86	Nanostructural Characteristics and Mechanical Properties of Low Temperature Plasma Enhanced Chemical Vapor Deposited Silicon Nitride Thin Films. Journal of Nanoscience and Nanotechnology, 2009, 9, 3734-3741.	0.9	6
87	HgCdTe technology in Australia. Proceedings of SPIE, 2009, , .	0.8	1
88	Design and Characterization of Fabry–Pérot MEMS-Based Short-Wave Infrared Microspectrometers. Journal of Electronic Materials, 2008, 37, 1811-1820.	2.2	27
89	Materials and Processes for MEMS-Based Infrared Microspectrometer Integrated on HgCdTe Detector. IEEE Journal of Selected Topics in Quantum Electronics, 2008, 14, 1031-1041.	2.9	11
90	Sidewall effects of MBE grown CdTe for MWIR HgCdTe photoconductors. Optoelectronic and Microelectronic Materials and Devices (COMMAD), Conference on, 2008, , .	0.0	0

#	Article	IF	CITATIONS
91	Widely tunable Fabry-Perot optical filter using fixed-fixed beam actuators. , 2008, , .		3
92	Laser beam induced current for qualitative evaluation of HgCdTe van der Pauw sample uniformity. Optoelectronic and Microelectronic Materials and Devices (COMMAD), Conference on, 2008, , .	0.0	0
93	Various annealing methods for activation of arsenic in Molecular Beam Epitaxy grown HgCdTe. Optoelectronic and Microelectronic Materials and Devices (COMMAD), Conference on, 2008, , .	0.0	0
94	Effect of heat treatment on internal stresses in PECVD SiN <inf>x</inf> H <inf>y</inf> thin films. Optoelectronic and Microelectronic Materials and Devices (COMMAD), Conference on, 2008, , .	0.0	0
95	MEMS-based tunable Fabry-Perot filters on silicon substrates. Optoelectronic and Microelectronic Materials and Devices (COMMAD), Conference on, 2008, , .	0.0	4
96	HgCdTe MWIR PECVD SiN passivated photodiodes. Optoelectronic and Microelectronic Materials and Devices (COMMAD), Conference on, 2008, , .	0.0	0
97	Incorporation and activation of arsenic in MBE-grown HgCdTe. Semiconductor Science and Technology, 2008, 23, 015014.	2.0	10
98	OPTICAL MEMS TECHNOLOGIES FOR ELECTRICALLY TUNABLE MULTI-SPECTRAL SHORT-WAVE INFRARED SENSORS AND ARRAYS. International Journal of High Speed Electronics and Systems, 2008, 18, 1035-1044.	0.7	3
99	MWIR HgCdTe Photodiodes based on high-density plasma-induced type conversion. Semiconductor Science and Technology, 2008, 23, 095027.	2.0	9
100	Real-time mass spectroscopy of reflected fluxes during molecular beam epitaxy growth of HgCdTe. Journal of Vacuum Science & Technology B, 2008, 26, 1068.	1.3	1
101	Recent developments in MEMS-based tunable IR detectors. , 2008, , .		0
102	Arsenic δ-doped HgTeâ^•HgCdTe superlattices grown by molecular beam epitaxy. Applied Physics Letters, 2008, 92, 082107.	3.3	9
103	Cross-flow microfiltration for lab-on-chip defatting of human breast milk. Proceedings of SPIE, 2008, ,	0.8	0
104	Poisson's Ratio of Low-Temperature PECVD Silicon Nitride Thin Films. Journal of Microelectromechanical Systems, 2007, 16, 622-627.	2.5	26
105	Process condition dependence of mechanical and physical properties of silicon nitride thin films. Journal of Applied Physics, 2007, 102, 103517.	2.5	10
106	Photoluminescence ofHgTeâ^•Hg1â^'xCdxTesuperlattices and a study of minibands. Physical Review B, 2007, 75, .	3.2	9
107	MEMS-based microspectrometers for infrared sensing. , 2007, , .		3

108 Crystallization and compositional changes in amorphous PECVD SiN x thin films. , 2007, , .

1

#	Article	IF	CITATIONS
109	Mechanical characteristics of filter structures for MEMS adaptive infrared detectors. , 2007, , .		Ο
110	Fabry-Perot MEMS microspectrometers spanning the SWIR and MWIR. , 2007, , .		2
111	1/f noise in HgCdTe infrared gated photodiodes. , 2007, , .		0
112	Extending the tuning range of SWIR microspectrometers. , 2007, , .		6
113	Micro-electromechanical systems-based microspectrometers covering wavelengths from 1500nm to 5000nm. , 2007, , .		4
114	Oxidation of PECVD SiNx thin films. Journal of Alloys and Compounds, 2007, 437, 332-338.	5.5	12
115	Annealing of C60o gamma radiation-induced damage in n-GaN Schottky barrier diodes. Journal of Applied Physics, 2007, 101, 054511.	2.5	17
116	Dielectric thin films for MEMS-based optical sensors. Microelectronics Reliability, 2007, 47, 733-738.	1.7	14
117	Crystallization of silicon nitride thin films synthesized by plasma-enhanced chemical vapour deposition. Scripta Materialia, 2007, 57, 739-742.	5.2	13
118	Magneto-Transport Characterization of p-Type HgCdTe. Journal of Electronic Materials, 2007, 36, 826-831.	2.2	8
119	Optical and Structural Properties of CdTe Grown by Molecular Beam Epitaxy at Low Temperature for Resonant-Cavity-Enhanced HgCdTe Detectors. Journal of Electronic Materials, 2007, 36, 877-883.	2.2	Ο
120	Investigation of 1/f Noise Mechanisms in Midwave Infrared HgCdTe Gated Photodiodes. Journal of Electronic Materials, 2007, 36, 884-889.	2.2	17
121	Effect of High-Density Plasma Process Parameters on Carrier Transport Properties in p-to-n Type Converted Hg0.7Cd0.3Te Layer. Journal of Electronic Materials, 2007, 36, 913-918.	2.2	12
122	Dark current modelling of midwave infrared HgCdTe gated photodiodes. , 2006, , .		3
123	Optical Performance of a MEMS Tunable IR Microspectrometer. , 2006, , .		Ο
124	Annealing and Shunting in RCE HgCdTe Photoconductors. , 2006, , .		0
125	High density plasma processing of p-Hg <inf>0.7</inf> Cd <inf>0.3</inf> Te. , 2006, , .		1
126	Design and optimisation of a MEMS-based tunable Fabry-Pérot infrared filter. , 2006, , .		1

#	Article	IF	CITATIONS
127	Thermal Stability of PECVD SiN/sub x/ Films. , 2006, , .		1
128	Characterisation of arsenic doped HgCdTe grown by Molecular Beam Epitaxy. , 2006, , .		1
129	Strain and orientation effects in mercury cadmium telluride grown by molecular beam epitaxy. , 2006, ,		0
130	Optical characterization of Fabry-Pe/spl acute/rot MEMS filters integrated on tunable short-wave IR detectors. IEEE Photonics Technology Letters, 2006, 18, 1079-1081.	2.5	26
131	Doubly-Supported Beam Actuators for MEMS-based Tunable Fabry-Perot Etalons. , 2006, , .		0
132	Resonant-cavity-enhanced HgCdTe photodetectors. , 2006, , .		0
133	SWIR hyperspectral detection with integrated HgCdTe detector and tunable MEMS filter. , 2006, 6295, 113.		9
134	Carrier transport characterization of high-density plasma-induced p-to-n type converted MWIR HgCdTe material. , 2006, , .		0
135	Tunable Fabry-Perot filters operating in the 3 to 5 \hat{l} $\!\!\!/4$ m range for infrared micro-spectrometer applications. , 2006, 6186, 69.		9
136	Adaptive focal plane array (AFPA) technologies for integrated infrared microsystems. , 2006, 6232, 70.		9
137	Effect of deposition conditions on mechanical properties of low-temperature PECVD silicon nitride films. Materials Science & Engineering A: Structural Materials: Properties, Microstructure and Processing, 2006, 435-436, 453-459.	5.6	161
138	Responsivity and lifetime of resonant-cavity-enhanced HgCdTe detectors. Solid-State Electronics, 2006, 50, 1640-1648.	1.4	9
139	Determination of HgCdTe elasto-plastic properties using nanoindentation. Journal of Electronic Materials, 2006, 35, 1197-1205.	2.2	6
140	Investigation of HgTe-HgCdTe superlattices by high-resolution X-ray diffraction. Journal of Electronic Materials, 2006, 35, 1481-1486.	2.2	5
141	Interpretation of current flow in photodiode structures using laser beam-induced current for characterization and diagnostics. IEEE Transactions on Electron Devices, 2006, 53, 23-31.	3.0	33
142	Stress in low-temperature plasma enhanced chemical vapour deposited silicon nitride thin films. Smart Materials and Structures, 2006, 15, S29-S38.	3.5	36
143	Effect of oxidation on the chemical bonding structure of PECVD SiNx thin films. Journal of Applied Physics, 2006, 100, 123516.	2.5	29
144	Responsivity and Lifetime of Resonant-cavity-enhanced HgCdTe photodetectors. , 2006, , .		0

#	Article	IF	CITATIONS
145	Environmental stability and cryogenic thermal cycling of low-temperature plasma-deposited silicon nitride thin films. Journal of Applied Physics, 2006, 99, 053519.	2.5	18
146	Nano-Porous Silicon antireflection coatings for microlens application. , 2006, , .		0
147	Structural Materials for NEMS/MEMS Devices. , 2006, , .		0
148	CHARACTERISTICS OF LOW TEMPERATURE PECVD SILICON NITRIDE FOR MEMS STRUCTURAL MATERIALS. International Journal of Modern Physics B, 2006, 20, 3799-3804.	2.0	4
149	Determination of mechanical properties of silicon nitride thin films using nanoindentation. , 2005, 5798, 216.		12
150	MEMS based tunable infrared sensors (Invited Paper). , 2005, 5840, 91.		0
151	Characterization of Electrically Active Defects in Photovoltaic Detector Arrays Using Laser Beam-Induced Current. IEEE Transactions on Electron Devices, 2005, 52, 2163-2174.	3.0	25
152	Mercury cadmium telluride/cadmium telluride distributed bragg reflectors for use with resonant cavity-enhanced detectors. Journal of Electronic Materials, 2005, 34, 710-715.	2.2	14
153	A monolithically integrated HgCdTe short-wavelength infrared photodetector and micro-electro-mechanical systems-based optical filter. Journal of Electronic Materials, 2005, 34, 716-721.	2.2	12
154	High-resolution X-ray diffraction studies of molecular beam epitaxy-grown HgCdTe heterostructures and CdZnTe substrates. Journal of Electronic Materials, 2005, 34, 795-803.	2.2	11
155	Effect of 60 Co gamma-irradiation on two-dimensional electron gas transport and device characteristics of AlGaN/GaN HEMTs. Physica Status Solidi C: Current Topics in Solid State Physics, 2005, 2, 2581-2584.	0.8	6
156	Nanoindentation of HgCdTe prepared by molecular beam epitaxy. Applied Physics Letters, 2005, 87, 251905.	3.3	28
157	Investigation of laser beam-induced current techniques for heterojunction photodiode characterization. Journal of Applied Physics, 2005, 98, 034501.	2.5	5
158	Generation-recombination effects on dark currents in CdTe-passivated midwave infrared HgCdTe photodiodes. Journal of Applied Physics, 2005, 98, 014504.	2.5	36
159	Effects of deposition temperature on the mechanical and physical properties of silicon nitride thin films. Journal of Applied Physics, 2005, 98, 044904.	2.5	28
160	A monolithically integrated HgCdTe SWIR photodetector and tunable MEMS-based optical filter. , 2005, 5783, 719.		6
161	Monolithic integration of an infrared photon detector with a MEMS-based tunable filter. IEEE Electron Device Letters, 2005, 26, 888-890.	3.9	54
162	Resonant cavity enhanced HgCdTe detectors. , 2005, , .		0

Resonant cavity enhanced HgCdTe detectors. , 2005, , . 162

#	Article	IF	CITATIONS
163	Evaluation of plasma deposited silicon nitride thin films for microsystems technology. Journal of Microelectromechanical Systems, 2005, 14, 971-977.	2.5	6
164	Mercury cadmium telluride resonant-cavity-enhanced photoconductive infrared detectors. Applied Physics Letters, 2005, 87, 211104.	3.3	26
165	Short-wavelength infrared tuneable filters on HgCdTe photoconductors. Optics Express, 2005, 13, 9683.	3.4	9
166	Determination of mechanical properties of PECVD silicon nitride thin films for tunable MEMS Fabry–Pérot optical filters. Journal of Micromechanics and Microengineering, 2005, 15, 608-614.	2.6	71
167	Chemical structure of low-temperature plasma-deposited silicon nitride thin films. , 2004, , .		3
168	Contribution of hole trap to persistent photoconductivity inn-type GaN. Journal of Applied Physics, 2004, 96, 1019-1023.	2.5	18
169	Optical quenching of photoconductivity in undopedn-GaN. Journal of Applied Physics, 2004, 95, 1081-1088.	2.5	11
170	The effects of vacuum baking on the I-V characteristics of LWIR HgCdTe photodiodes. , 2004, , .		2
171	Correlation of laser-beam-induced current with current-voltage measurements in HgCdTe photodiodes. Journal of Electronic Materials, 2004, 33, 560-571.	2.2	12
172	Laser-beam-induced current mapping of spatial nonuniformities in molecular beam epitaxy As-grown HgCdTe. Journal of Electronic Materials, 2004, 33, 572-578.	2.2	6
173	Resonant cavity-enhanced mercury cadmium telluride detectors. Journal of Electronic Materials, 2004, 33, 604-608.	2.2	7
174	Dark currents in long wavelength infrared HgCdTe gated photodiodes. Journal of Electronic Materials, 2004, 33, 621-629.	2.2	23
175	Uniformity in HgCdTe diode arrays fabricated by reactive ion etching. Journal of Electronic Materials, 2004, 33, 141-145.	2.2	2
176	Low temperature saturation of p–n junction laser beam induced current signals. Solid-State Electronics, 2004, 48, 409-414.	1.4	21
177	Characterization of crosstalk in HgCdTe n-on-p photovoltaic infrared arrays. , 2004, , .		6
178	Magnetoresistance characteristics of gamma-irradiated Al 0.35 Ga 0.65 N/GaN HFETs. , 2004, 5274, 152.		0
179	Refractive index engineering for a distributed Bragg reflector for a resonant-cavity-enhanced detector. , 2004, , .		0
180	Determination of residual stress in low-temperature PECVD silicon nitride thin films. , 2004, 5276, 451.		11

#	Article	IF	CITATIONS
181	Accurate determination of composition profiles in abrupt MBE-grown HgCdTe heterostructures. , 2004, , .		2
182	HgCdTe long-wavelength infrared photovoltaic detectors fabricated using plasma-induced junction formation technology. Journal of Electronic Materials, 2003, 32, 615-621.	2.2	15
183	Planar p-on-n HgCdTe heterojunction mid-wavelength infrared photodiodes formed using plasma-induced junction isolation. Journal of Electronic Materials, 2003, 32, 622-626.	2.2	13
184	Small two-dimensional arrays of mid-wavelength infrared HgCdTe diodes fabricated by reactive ion etching-induced p-to-n-type conversion. Journal of Electronic Materials, 2003, 32, 627-632.	2.2	17
185	Minority carrier lifetime and noise in abrupt molecular-beam epitaxy-grown HgCdTe heterostructures. Journal of Electronic Materials, 2003, 32, 639-645.	2.2	4
186	/sup 60/Co gamma irradiation effects on n-GaN Schottky diodes. IEEE Transactions on Electron Devices, 2003, 50, 2326-2334.	3.0	96
187	Noise modeling in HgCdTe heterostructure devices. Journal of Applied Physics, 2003, 94, 6541-6548.	2.5	1
188	HgCdTe long-wavelength infrared photovoltaic detectors formed by reactive ion etching. , 2002, 4795, 146.		0
189	Minority carrier lifetime in abrupt MBE grown HgCdTe heterostructures. , 2002, , .		0
190	Towards MEMS-based infrared tunable microspectrometers. , 2002, 4935, 148.		11
191	60Co gamma-irradiation-induced defects in n-GaN. Applied Physics Letters, 2002, 80, 4354-4356.	3.3	66
192	Transport properties of reactive-ion-etching-induced p-to-n type converted layers in HgCdTe. Journal of Electronic Materials, 2002, 31, 652-659.	2.2	22
193	Passivation effects on reactive-ion-etch-formed n-on-p junctions in HgCdTe. Journal of Electronic Materials, 2002, 31, 743-748.	2.2	14
194	Mechanochemical Synthesis and Characterization of GaN Nanocrystals. Journal of Nanoparticle Research, 2002, 4, 367-371.	1.9	9
195	<title>60Co gamma-irradiation-induced defects in MOCVD n-GaN</title> . , 2001, , .		1
196	<title>Mobility spectrum techniques for characterizing multilayer semiconductor structures</title> . , 2001, , .		0
197	RIE-induced n-on-p junction HgCdTe photodiodes: effects of passivant technology on bake stability. , 2001, 4454, 106.		2
198	Diffusion length measurements in p-HgCdTe using laser beam induced current. Journal of Electronic Materials, 2001, 30, 696-703.	2.2	26

#	Article	IF	CITATIONS
199	p-to-n type-conversion mechanisms for HgCdTe exposed to H2/CH4 plasmas. Journal of Electronic Materials, 2001, 30, 762-767.	2.2	27
200	Effects of Band Tail Absorption on AlGaN-Based Ultraviolet Photodiodes. Physica Status Solidi A, 2001, 188, 311-315.	1.7	0
201	Tunable Fabry-Pérot cavities fabricated from PECVD silicon nitride employing zinc sulphide as the sacrificial layer. Journal of Micromechanics and Microengineering, 2001, 11, 589-594.	2.6	46
202	A simplified fabrication process for HgCdTe photoconductive detectors using CH4/H2reactive-ion-etching-induced blocking contacts. Semiconductor Science and Technology, 2001, 16, 455-462.	2.0	5
203	<title>Tunable Fabry-Perot cavities</title> ., 2000, , .		4
204	Characterisation of dark current in novel Hg1â^'xCdxTe mid-wavelength infrared photovoltaic detectors based on n-on-p junctions formed by plasma-induced type conversion. Journal of Crystal Growth, 2000, 214-215, 1106-1110.	1.5	10
205	Transferable silicon nitride microcavities. Microelectronics Journal, 2000, 31, 523-529.	2.0	4
206	Laser beam induced current as a tool for HgCdTe photodiode characterisation. Microelectronics Journal, 2000, 31, 537-544.	2.0	20
207	Anomalous drain current–voltage characteristics in AlGaN/GaN MODFETs at low temperatures. Microelectronics Journal, 2000, 31, 531-536.	2.0	1
208	HgCdTe photovoltaic detectors fabricated using a new junction formation technology. Microelectronics Journal, 2000, 31, 545-551.	2.0	11
209	Characterization of Hg0.7Cd0.3Te n- on p-type structures obtained by reactive ion etching induced p- to n conversion. Journal of Electronic Materials, 2000, 29, 837-840.	2.2	36
210	HgCdTe mid-wavelength IR photovoltaic detectors fabricated using plasma induced junction technology. Journal of Electronic Materials, 2000, 29, 841-848.	2.2	53
211	H2-based dry plasma etching for mesa structuring of HgCdTe. Journal of Electronic Materials, 2000, 29, 853-858.	2.2	10
212	Scattering mechanisms limiting two-dimensional electron gas mobility in Al0.25Ga0.75N/GaN modulation-doped field-effect transistors. Journal of Applied Physics, 2000, 87, 3900-3904.	2.5	126
213	Junction depth measurement in HgCdTe using laser beam induced current (LBIC). Journal of Electronic Materials, 1999, 28, 603-610.	2.2	29
214	Analysis of crosstalk in HgCdTe p-on-n heterojunction photovoltaic infrared sensing arrays. Journal of Electronic Materials, 1999, 28, 617-623.	2.2	24
215	Near band-edge field-dependent absorption coefficient and refractive index determined by photocurrent and transmittance measurements. Applied Optics, 1999, 38, 5127.	2.1	2
216	<title>Laser-beam-induced current technique as a quantitative tool for HgCdTe photodiode</td><td></td><td>3</td></tr></tbody></table></title>		

characterization</title>., 1999, , .

#	Article	IF	CITATIONS
217	<title>Excess noise in MWIR photovoltaic detectors fabricated using a new junction formation technology</title> . , 1999, 3892, 221.		0
218	<title>Anomalous drain current-voltage characteristics in AlGaN/GaN MODFETs at low
temperatures</title> . , 1999, , .		2
219	<title>Transferable silicon nitride microcavities</title> ., 1999, 3892, 142.		1
220	Design of externally tuned asymmetric fibre Fabry–Perot electroabsorption optical modulators. IEE Proceedings: Optoelectronics, 1998, 145, 344-352.	0.8	4
221	Laser beam induced current imaging of reactive ion etching induced n-type doping in HgCdTe. Journal of Electronic Materials, 1998, 27, 661-667.	2.2	10
222	Multi-heterojunction large area HgCdTe long wavelength infrared photovoltaic detector for operation at near room temperatures. Journal of Electronic Materials, 1998, 27, 740-746.	2.2	26
223	Mercury annealing of reactive ion etching induced p- to n-type conversion in extrinsically doped p-type HgCdTe. Journal of Applied Physics, 1998, 83, 5555-5557.	2.5	18
224	Simulation of mid-infrared HgTe/CdTe quantum-well vertical-cavity surface-emitting lasers. Journal of Applied Physics, 1998, 83, 4286-4291.	2.5	11
225	Estimation of doping density in HgCdTe p-n junctions using scanning laser microscopy. Applied Physics Letters, 1998, 72, 52-54.	3.3	19
226	A novel multi-heterojunction HgCdTe long-wavelength infrared photovoltaic detector for operation under reduced cooling conditions. Semiconductor Science and Technology, 1998, 13, 1209-1214.	2.0	21
227	Wide optical bandwidth asymmetric Fabry–Pérot reflection modulator using the quantum confined Stark effect. Journal of Applied Physics, 1998, 84, 5761-5765.	2.5	10
228	Scanning laser microscopy of reactive ion etching inducedn-type conversion in vacancy-dopedp-type HgCdTe. Applied Physics Letters, 1997, 70, 3443-3445.	3.3	19
229	<title>Isothermal vapor phase epitaxy as a versatile technology for infrared photodetectors</title> . , 1997, 2999, 34.		11
230	Magnetic field dependent Hall data analysis of electron transport in modulation-doped AlGaN/GaN heterostructures. Journal of Applied Physics, 1997, 82, 2996-3002.	2.5	47
231	A monolithic dual-band HgCdTe infrared detector structure. IEEE Electron Device Letters, 1997, 18, 352-354.	3.9	3
232	Evaluation of III–V multilayer transport parameters using quantitative mobility spectrum analysis. Materials Science and Engineering B: Solid-State Materials for Advanced Technology, 1997, 44, 65-69.	3.5	16
233	<title>Long-wavelength infrared photoconductor technology based on epitaxially grown
Hg<formula><inf><roman>1-x</roman></inf></formula>Cd<formula><inf><roman>x</roman></inf></formula>
, 1995, , .</td><td>ſe</title> .	0	
234	<title>Status of MWIR HgCdTe photovoltaic detector technology in Australia</title> . , 1995, 2552, 110.		0

#	Article	IF	CITATIONS
235	<title>Erasure of poling-induced second-order optical nonlinearities in silica by UV exposure</title> . , 1994, 2289, 185.		12
236	Multiple-quantum-well reflection modulator using a lifted-off GaAs/AlGaAs film bonded to gold on silicon. Electronics Letters, 1991, 27, 557.	1.0	8
237	Strain effects in chemically lifted GaAs thin films. Physical Review B, 1990, 41, 7749-7754.	3.2	7
238	Unusually strong excitonic absorption in molecular-beam-epitaxy-grown, chemically lifted GaAs thin films. Physical Review B, 1990, 42, 9496-9500.	3.2	8
239	Dependence of ohmic contact quality on Au-Ge alloy-thickness for n-type GaAs. International Journal of Electronics, 1984, 57, 729-736.	1.4	7
240	Auî—ʿGeî—ʿNi migration affected by operating conditions of GaAs FETs. Solid-State Electronics, 1984, 27, 447-452.	1.4	7
241	Some new concepts of heat-flow spreading in GaAs FET structures. International Journal of Electronics, 1984, 57, 155-160.	1.4	6
242	Ultrathin-film ohmic contacts for GaAs FET. Journal Physics D: Applied Physics, 1983, 16, L243-L245.	2.8	5
243	A bistable MOSFET-type metal-tunnel insulator-semiconductor switch. IEEE Electron Device Letters, 1981, 2, 121-122.	3.9	4
244	Charge trapping centres in \hat{I}^3 -irradiated Gallium Nitride grown by MOCVD. , 0, , .		0
245	Towards a laser beam induced current test structure for the nondestructive determination of junction depth in HgCdTe photodiodes. , 0, , .		1
246	Finite element analysis of tunable Fabry Perot MEMS structures. , 0, , .		4
247	Modelling output admittance frequency dispersion in AlGaN/GaN MODFETs. , 0, , .		0
248	Diffusion length measurements using laser beam induced current. , 0, , .		1
249	Nano-indentation characterisation of PECVD silicon nitride films. , 0, , .		3
250	Hydrogenation of ZnS passivation for HgCdTe. , 0, , .		0
251	Stress relaxation mechanisms in mismatched epitaxial growth of HgCdTe. , 0, , .		0

An inexpensive midwave infrared HgCdTe camera. , 0, , .

0

#	Article	IF	CITATIONS
253	Characterisation of reactive ion etching induced type conversion in HgCdTe. , 0, , .		0
254	Kinetics of persistent photoconductivity in GaN grown by MOCVD. , 0, , .		0
255	Temperature stability of HgCdTe n-on-p junctions formed by reactive ion etching. , 0, , .		0
256	Nondestructive determination of p-n junction depth using laser beam induced current and lateral photovoltage measurements. , 0, , .		0
257	Variable MEMS-based inductors fabricated from PECVD silicon nitride. , 0, , .		6
258	Minority carrier behaviour in abrupt MBE grown HgCdTe heterostructures. , 0, , .		0
259	Modelling of dark currents in LWIR HgCdTe photodiodes. , 0, , .		0
260	Non-contact evaluation of photodiode performance by laser beam induced current imaging. , 0, , .		1
261	Small HgCdTe infrared detector arrays from UWA. , 0, , .		Ο
262	Characterisation of MBE Grown HgCdTe Using Scanning Laser Microscopy. , 0, , .		0
263	Mercury Cadmium Telluride/Cadmium Telluride Distributed Bragg Reflectors. , 0, , .		0
264	Stress Response of Low Temperature PECVD Silicon Nitride Thin Films to Cryogenic Thermal Cycling. , 0, , .		4
265	Investigation of Surface Passivation of HgCdTe MWIR Photodiode Arrays via a Flood Illumination Technique. , 0, , .		1
266	Reciprocal Space Mapping of MBE-Grown HgCdTe Heterostructures. , 0, , .		0
267	Structural and Optical Characterisation of. , 0, , .		0
268	Mechanical Design and Finite Element Analysis of Tunable Fabry-Perot MEMS Structures for Adaptive Infrared Detectors. , 0, , .		1
269	Strain Evaluation of Plasma-Deposited Silicon Nitride. , 0, , .		0